Research Article Vol. 30, No. 1 / 3 Jan 2022 / Optics Express 349
Optics EXPRESS

Simultaneous film thickness and refractive index measurement using a constrained fitting method in a white light spectral interferometer

LIN YUAN,[1] TONG GUO,[1,*] DAWEI TANG,[2] HAITAO LIU,[3,4] AND XINYUAN GUO[1]

[1]State Key Laboratory of Precision Measuring Technology and Instruments, Tianjin University, Tianjin 300072, China
[2]Centre for Precision Technologies, University of Huddersfield, Huddersfield, UK
[3]Institute of Modern Optics, College of Electronic Information and Optical Engineering, Nankai University, Tianjin 300350, China
[4]Tianjin Key Laboratory of Micro-scale Optical Information Science and Technology, Tianjin 300350, China
*guotong@tju.edu.cn

Abstract: Film is widely used in optoelectronic and semiconductor industries. The accurate measurement of the film thickness and refractive index, as well as the surface topography of the top and bottom surfaces are necessary to ensure its processing quality. Multiple measurement methods were developed; however, they are limited by the requirements of a known dispersion model and initial values of thickness and refractive index. Further, their systems are rarely compatible with surface topography measurement methods. We propose a constrained nonlinear fitting method to simultaneously measure the thickness and refractive index of film in a simple white-light spectral interferometer. The nonlinear phase extracted by the spectral phase-shifting is fitted with the theoretical nonlinear phase obtained by multiple reflection model. The constraints of nonlinear fitting are obtained by the interferometric signal of vertical scanning, reconstructed by the integration of the white-light spectral signal to avoid local minima. The proposed method does not require a priori knowledge of the dispersion model and initial values of thickness and refractive index, and its system is compatible with the vertical scanning interferometry (VSI) method to reconstruct the surface topography of the top and bottom surfaces of film. Three SiO_2 films with different thicknesses are measured, and the results show that the measured refractive index is within the theoretical value range of wavelength bandwidth and the measured thicknesses are closely aligned with the values provided by the commercial instrument. The measurement repeatability of refractive index reaches 10^{-3}. Measurements on a polymer film demonstrate that this method is feasible for measuring the film without a priori information.

1. Introduction

Film has an increasing number of applications in the fields of optoelectronics and semiconductors. Numerous novel film materials with excellent performance are continuously being produced. Polymer films with high stability are used to encapsulate the wafer package instead of traditional materials [1–4]. Accurate measurement of the film thickness and refractive index, as well as the surface topography of top and bottom surfaces are necessary to ensure its processing quality. Optical measurement methods have been widely studied and applied due to their high accuracy and resolution, non-destructiveness, and rapid measurement. Ellipsometry and reflectometry [5–8] are usually considered as the most reliable and commercially available methods to determine the thickness and refractive index due to their high accuracy, which requires a priori knowledge of the dispersion model and initial values of the thickness and refractive index. However, the

#447830 https://doi.org/10.1364/OE.447830
Journal © 2022 Received 5 Nov 2021; revised 6 Dec 2021; accepted 6 Dec 2021; published 21 Dec 2021

Optics EXPRESS

dispersion models of some novel film materials are unknown, or do not belong to the known dispersion model, and the initial values of thickness and refractive index are difficult to obtain. Therefore, the application of these measurement methods is limited. Furthermore, their systems are difficult to make compatible with surface topography measurement methods.

White-light interferometry is widely used in film measurement. The vertical scanning interferometry (VSI) method is implemented when a camera receives the interferometric signal, which is widely used to reconstruct the surface topography of top and bottom surfaces of film with a known refractive index. For the simultaneous measurement of thickness and refractive index, some methods perform the Fourier transform on the interferometric signal of the VSI method [9–11]. Then, the reflectance spectrum is accessed from the amplitude of the Fourier transform. Thus, these methods can realize the simultaneous measurement of thickness, refractive index, and surface topography of the top and bottom surfaces of film. The measurement results of the thickness and refractive index have an error below 1% compared to the ellipsometry results [11]. However, they have the same application limitation as reflectometry, namely the requirements of a known dispersion model and initial values of thickness and refractive index. In the method proposed by *Lee et al.* [10], the interferometric signal of vertical scanning is used for the Fourier transform only contains the signal when the scanning position is close to the top surface, where the signal from bottom surface of the film is ideally equivalent to a fixed value. Hence, the reflectance spectrum calculated by the Fourier transform is composed of the reflection coefficient for the film-air interface, such that the dispersion model is not required for fitting. *Kitagawa et al.* [12] constructed a three-wavelength interferometric imaging system, including a three-wavelength (B, G, R) illumination and a color camera. The theoretical model of interferometric signal of vertical scanning is expressed as the sum of two sinusoidal signals, one corresponding to the top surface, and one to the bottom surface. The interferometric signal of the three wavelengths (B, G, R) are nonlinearly fitted with the theoretical model to obtain the thickness and refractive index. The above methods require an accurate pre-calibration process, and the accuracy of scanner device, light source variation in time, and illumination nonuniformity [11] may affect the accurate acquisition of the interferometric signal, hence affecting the measurement accuracy.

The spectrometer is used in the interferometric system to implement the white-light spectral interferometry. For the transmission interferometry [13–18], the thickness and refractive index can usually be calculated according to the characteristics that the absolute distance can be extracted using white-light spectral interferometry. Generally, the equations are established by the absolute distance difference between the insertion and removal of the film in the optical path. Or other equipment (e.g., the Abbe refractometer and a micrometer with high resolution) is required to solve the phase ambiguity arising from the fact that the inverse trigonometric functions are multi-valued, which increases the complexity and uncertainty of measurement. Evidently, the film without substrate cannot be measured using transmission interferometry. *Ghim et al.* [19] constructed a white-light spectral interferometer with polarization optics to distinguish the spectral signal of the film itself and the spectral signals of film and reference mirror. Then, the Fourier transform was applied on the spectral signals to obtain absolute distances and establish equations. This method can realize the rapid measurement of thickness and refractive index, as there is no mechanical scanning process. However, the system structure is complex, with some polarization optics and two spectrometers. In nonlinear phase analysis methods [20–22], because the nonlinear phase is caused by multiple reflection of the film, so the extracted nonlinear phase can be fitted with the theoretical values to calculate the measured parameters. These methods exhibit good stability and accuracy, as the phase of the spectral signal is more stable than the intensity. However, these methods are mainly used to access the film thickness with a known refractive index, and there are requirements for the accuracy of the initial value of thickness for fitting.

Optics EXPRESS

We propose a constrained nonlinear fitting method for measuring the thickness and refractive index of film in a simple white-light spectral interferometer. The nonlinear phase is extracted by the spectral phase-shifting, and to avoid local minima when fitting the extracted nonlinear phase using the theoretical multiple reflection model, we introduce two fitting constraints obtained by the interferometric signal of vertical scanning reconstructed by the integration of the white-light spectral signal. Subsequently, the constrained nonlinear fitting process is described in detail. The factors affecting the fitting results are analyzed, mainly including the constraints accuracy and wavelength resolution. We measured three SiO_2 films with different thicknesses to verify the accuracy of the proposed method and evaluated the measurement repeatability. Furthermore, the measurement of a polymer film was carried out to demonstrate the feasibility of the proposed method.

2. Methodology

2.1. Mathematical model

The vector mathematical model of the spectral interferometric signal generated by the film is usually expressed as

$$\begin{aligned} S &= |E_r + E_m|^2 = |Ee^{-i(\omega t - kr_1)} + Ee^{-i(\omega t - kr_2)}R|^2 \\ &= E^2 + E^2|R|^2 + 2E^2|R|cos(\varphi + \arg(R)) \end{aligned}, \tag{1}$$

where E_r and E_m are the electric vectors of the beams respectively reflected from the reference mirror and the film in the measurement arm, r_1 and r_2 are the optical path lengths in air, R is the reflection coefficient of the film. The phase $\varphi + \arg(R)$ is the total phase distribution (Fig. 1(a)), which can be decomposed into the phase φ generated by the optical path difference in air between the reference and measuring beams (Fig. 1(b)), and the phase $\arg(R)$ generated by the multiple reflection of light inside the film. Thus, the nonlinear part in the total phase distribution is only related to the film, and we can remove the linear part from the total phase distribution to extract the nonlinear phase by applying a linear fitting, as shown in Fig. 1(c). In this study, we use a five-step phase-shifting algorithm to extract the total phase distribution [23].

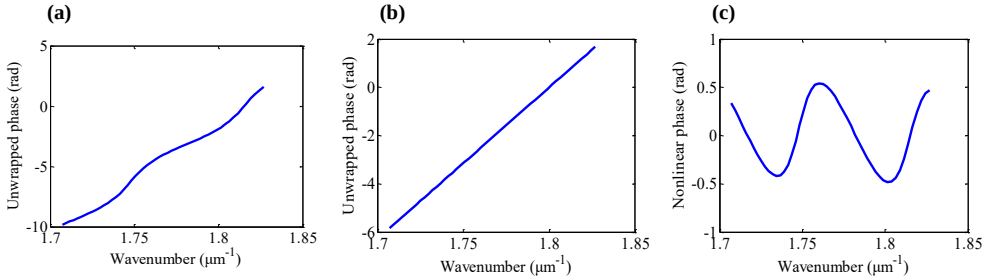

Fig. 1. (a) Total phase distribution $\varphi + \arg(R)$, (b) phase φ, and (c) nonlinear phase.

2.2. Nonlinear fitting process

The phase difference due to multiple reflection of the film with normal-incidence light is

$$\arg(R) = \arg\left(\frac{r_{01} + r_{12}\exp(i4\pi k n_1 d)}{1 + r_{01}r_{12}\exp(i4\pi k n_1 d)}\right), \tag{2}$$

where r_{01} and r_{12} are the Fresnel reflection coefficients for the film-air interface and film-substrate interface, respectively, k is the wavenumber, $n_1 = n + iK$ is the complex refractive index, and d is

Optics EXPRESS

the thickness. Because the nonlinear phase is only related to the film, the measured nonlinear phase can be fitted with the theoretical nonlinear phase obtained by the multiple reflection model. The Levenberg–Marquardt (L-M) least-squares method is used in this study for nonlinear fitting. In the proposed method, the optical constants are equivalent to effective values, which is reasonable because the wavelength bandwidth used for fitting is narrow and the influence of dispersion is weak. Meanwhile, the refractive index used in the VSI method to reconstruct the surface topography of the top and bottom surfaces of the film is likewise an effective value. To reduce the influence of dispersion of the film, a narrow wavelength bandwidth needs to be used. However, it should be noted that the corresponding nonlinear phase should contain at least one period to provide sufficient information for fitting. In this work, the corresponding nonlinear phase contains about 1~3 periods, depending on the material and thickness of the film.

The difficulty of nonlinear fitting is that the three parameters n, d, and K to be fitted are interrelated, i.e., not independent. Therefore, it is important to limit the nonlinear fitting process to avoid local minima. In this study, two constraints of nonlinear fitting are established. To start, we perform a vertical scanning on the film and record the spectral signal at each scanning step. The interferometric signal of the vertical scanning can be reconstructed by the integration of white-light spectral signal as follows

$$I_i = \int_{\lambda_1}^{\lambda_2} S_i(\lambda) d\lambda, i = 1, 2, 3 \ldots N, \tag{3}$$

where S_i is the recorded spectral signal, λ is the wavelength, and N is scanning steps. It should be noted that when the scanning position close to the top and bottom surfaces, the scanning step needs to be small enough to ensure accuracy. Afterwards, two constraints of nonlinear fitting are established from the reconstructed interferometric signal of vertical scanning.

2.2.1. Constraint 1

There are two coherence envelopes that can be detected in the reconstructed interferometric signal of vertical scanning, as shown in Fig. 2. We use gravity method to separately detect the accurate center position of coherence envelopes. Then, the measured optical thickness of film $T = nd$ is extracted, which is the Constraint 1 that limits the initial value of thickness d in the nonlinear fitting process.

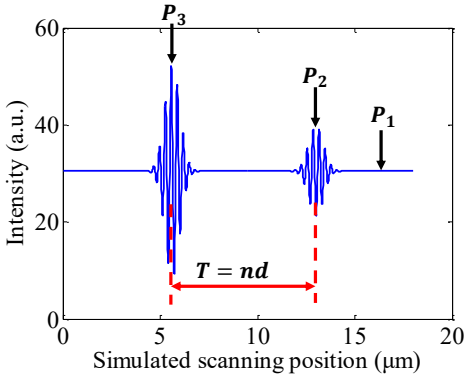

Fig. 2. Schematic diagram of two constraints.

2.2.2. Constraint 2

In the reconstructed interferometric signal of vertical scanning, the background light intensity P_1, envelope peak intensity of top surface P_2, and envelope peak intensity of bottom surface

Optics EXPRESS

P_3 all contain information about the thickness and optical constants of the film (Fig. 2). A Gaussian fitting method is employed to calculate the accurate envelope peak values, and their ratios $T_1 = P_2/P_1$ and $T_2 = (P_3 - P_1)/(P_2 - P_1)$ represent the Constraint 2 that limits the initial value of extinction coefficient K in the nonlinear fitting process. Specifically, this serves to calculate the solution of nonlinear equations

$$\begin{aligned} &\text{Nonlinear equation1}: \quad f_1(K) = \int_{\lambda_1}^{\lambda_2} \frac{|1 + r_{01}|^2 + |t_{01} r_{12} t_{10} \exp(i4\pi k n_1 d)|^2}{1 + |R|^2} d\lambda - T_1 = 0 \\ &\text{Nonlinear equation2}: \quad f_2(K) = \int_{\lambda_1}^{\lambda_2} \frac{|1 + t_{01} r_{12} t_{10}|^2 + |r_{01} \exp(-i4\pi k n_1 d)|^2 - (1 + |R|^2)}{|1 + r_{01}|^2 + |t_{01} r_{12} t_{10} \exp(i4\pi k n_1 d)|^2 - (1 + |R|^2)} d\lambda - T_2 = 0 \end{aligned}, \tag{4}$$

where t_{01} and t_{10} are the Fresnel transmission coefficients for the film-air interface, and $n_1 = n + iK$ is the complex refractive index.

2.2.3. Nonlinear fitting procedure

Step 1: The total phase distribution is accessed by a five-step phase-shifting algorithm, and the nonlinear phase is extracted by removing the linear part from the total phase distribution by applying linear fitting. Meanwhile, the nonlinear phase error caused by the system also must be eliminated [20].

Step 2: Reconstruct the interferometric signal by integrating the white-light spectral signals recorded in vertical scanning process. Then, the Constraint 1, measured optical thickness of film $T = nd$, and the Constraint 2, intensity ratios $T_1 = P_2/P_1$ and $T_2 = (P_3 - P_1)/(P_2 - P_1)$, are extracted.

Step 3: The measured nonlinear phase and theoretical nonlinear phase obtained by multiple reflection model are fitted with constraints in a fitting loop with an initial value of the refractive index. The fitting results with the minimum residual error are the final measurement results of the thickness and refractive index of film. More specifically, in each fitting loop, the initial values of thickness and extinction coefficient are determined according to constraints of nonlinear fitting, which works in avoiding local minima.

3. Analysis

3.1. Influence of constraints accuracy

The initial values of parameters to be fitted are determined according to the constraints to avoid local minima. Therefore, even if the initial values do not represent the final fitting results of the thickness and refractive index, they likewise have certain accuracy requirements. The gravity method is widely used in the coherence envelope detection in VSI method, such that the Constraint 1 has good accuracy and stability. However, due to the influence of the spectral envelope of the light source, misalignment or manufacturing errors of the beam splitter prism and other factors, the reconstructed interferometric signal of vertical scanning usually must be corrected to obtain an accurate Constraint 2. A pre-calibration step is carried out using a standard *Si* wafer. We also performed vertical scanning on the *Si* wafer and reconstructed interferometric signal by the integration of white-light spectral signal, as shown in Fig. 3(a). The background light intensity P_{Si-1} and envelope peak intensity P_{Si-2} also contains information about the refractive index of *Si*. The theoretical value of $T_{Si} = P_{Si-2}/P_{Si-1}$ is given as

$$T_{Si-Theoretical} = \int_{\lambda_1}^{\lambda_2} \frac{|1 + r_{Si}|^2}{1 + |r_{Si}|^2} d\lambda, \tag{5}$$

Optics EXPRESS

where r_{Si} is the Fresnel reflection coefficient for the *Si*-air interface, and the theoretical value of T_{Si} is 1.883. However, the measured value is usually inconsistent with the theoretical value; for example, the measured value in Fig. 3(a) is 1.740. Hence, in this study, the constant value C is used to correct the measured ratio value to equal the theoretical value (Fig. 3(b)):

$$T_{Si-Measured} = \frac{P_{Si-2} - C}{P_{Si-1} - C}, \tag{6}$$

The obtained constant value C is also applied to the subsequent measurements of Constraint 2 of film. The pre-calibration step only needs to be carried out again when the intensity of light source and exposure time of the spectrometer are changed.

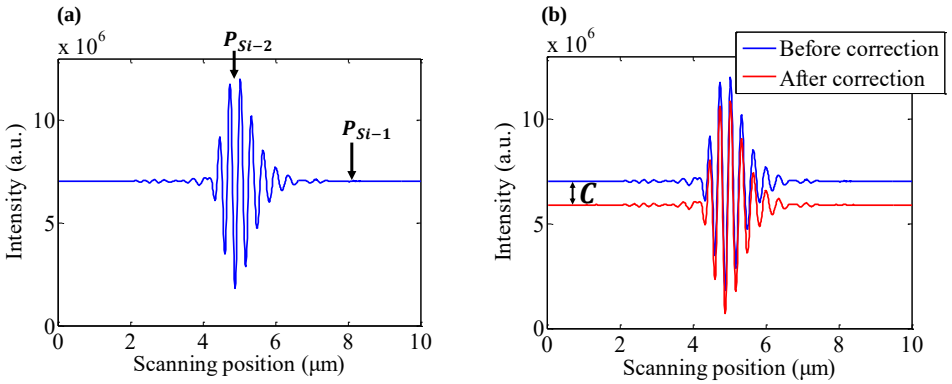

Fig. 3. (a) Reconstructed interferometric signal of vertical scanning of *Si* wafer, and (b) before and after correction.

We simulated the vertical scanning process with 10 nm steps on a SiO_2 film on *Si* substrate with a thickness of 5 μm, and reconstructed the interferometric signal of vertical scanning to analyze the influence of accuracy of Constraint 2. The theoretical values of T_1 and T_2 are 1.302 and 2.377, respectively. Generally, factors such as environmental noise and the scanning step may affect the envelope peak intensity, such that the values of T_1 and T_2 are less than the theoretical values. We simulated the different error percentages (0–10%) of T_1 and T_2, and as shown in Fig. 4, the fitting results of the refractive index are almost all within the error band of 1% of the theoretical value. This is because constraints limit the nonlinear fitting process to avoid local minima. The accurate measurement results are acquired by fitting the measured and theoretical nonlinear phases. It also can be seen that T_2 has a greater impact on the fitting results because T_2 is more sensitive to extinction coefficient than T_1. And we use two nonlinear equations to improve the robustness of Constraint 2.

We measured a SiO_2 film on *Si* substrate with the thickness of 5.017 μm measured by the commercial reflectometry instrument. The vertical scanning was repeated eight times with 10 nm steps when the scanning position is close to the top and bottom surfaces, and the interferometric signals of vertical scanning were reconstructed. The repeated measurement results of Constraint 2 are shown in Table 1, and the values of T_1 and T_2 exhibit good stability. The slight deviation of T_2 between the measured and theoretical values may be due to scattering inside the film. Therefore, it is necessary to ensure the uniformity in area and depth of the measured film to guarantee the constraint accuracy. Meanwhile, the optical thickness of the film must be larger than the coherence length of the light source to avoid overlap between the envelopes of top and bottom surfaces.

Optics EXPRESS

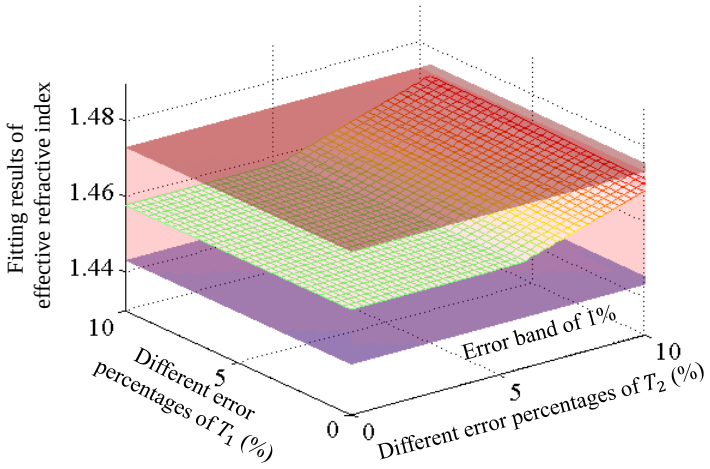

Fig. 4. Fitting results of refractive index at different error percentages of T_1 and T_2.

Table 1. Repeated measurement results of Constraint 2

	$T_1 = P_2/P_1$	$T_2 = (P_3 - P_1)/(P_2 - P_1)$
Mean	1.299	2.339
Standard deviation	0.002	0.010

3.2. *Influence of wavelength resolution*

The wavelength resolution mainly affects the intensity of spectral signal, i.e., the integral average effect. To further illustrate this, we measured a plane mirror and performed a five-step phase-shifting algorithm to extract the absolute distances. We compared the contrast of spectral signals with at least one period at different absolute distance positions and spectral signals at absolute distances of 5.1 μm and 25.1 μm. The contrast can be computed as

$$Contrast = \frac{S_{\max} - S_{\min}}{S_{\max} + S_{\min}}, \tag{7}$$

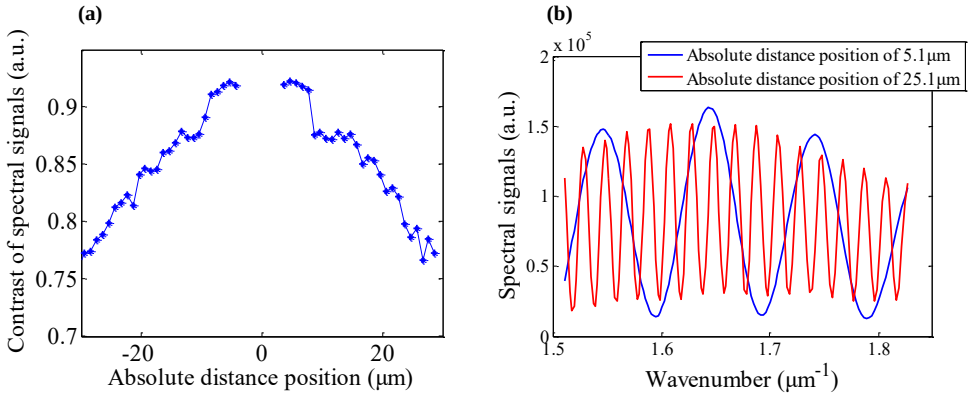

Fig. 5. (a) Contrast of spectral signals at different absolute distance positions, and (b) spectral signals at two different absolute distance positions.

Optics EXPRESS

Table 2. Fitting results with different wavelength resolutions at different measuring positions in simulation

Measuring position	Effective refractive index n_{eff}		Measured thickness d (μm)	
	λ_{Res} =0.1 nm	λ_{Res} =0.8 nm	λ_{Res} =0.1 nm	λ_{Res} =0.8 nm
Position 1	1.457	1.449	5.004	5.032
Position 2	1.457	1.456	5.004	5.008
Position 3	1.457	1.461	5.004	4.991

where S_{max} and S_{min} are the maximum and minimum intensities of the spectral signal. As shown in Fig. 5(a), the contrast decreases gradually as the absolute distance position moves away from the zero optical path difference position. The reason is that the spectral signals away from the zero optical path difference position contain more periods, and the integral average effect of wavelength resolution has a stronger influence on the spectral signals with more periods (Fig. 5(b)).

Theoretically, the nonlinear phase is generated by multiple reflection of light inside the film, which is independent of the experimental parameters. However, the integral average effect of wavelength resolution may affect the spectral intensity of the five-step phase-shifting algorithm,

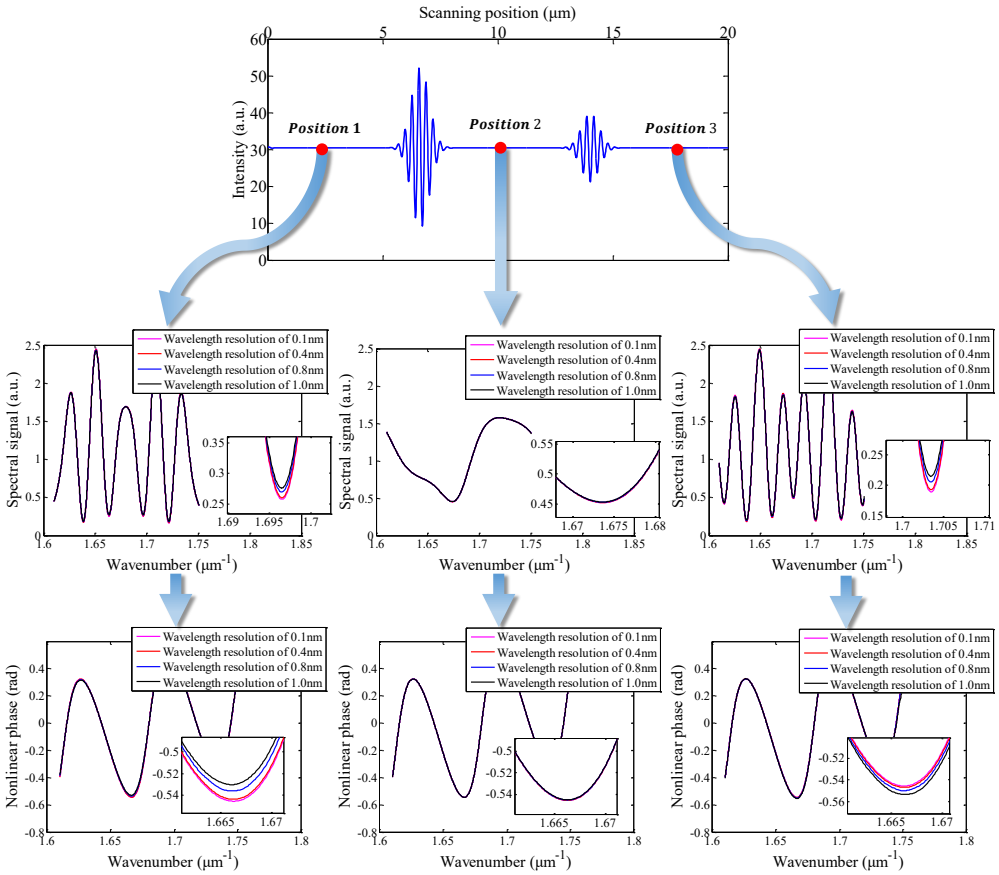

Fig. 6. Nonlinear phases with different wavelength resolutions at different measuring positions in simulation.

Optics EXPRESS

and then influence the extracted nonlinear phase. We simulated the measurement of a SiO_2 film on Si substrate with thickness of 5 μm, and we performed a five-step phase-shifting algorithm with different wavelength resolutions (0.1 nm, 0.4 nm, 0.8 nm, and 1.0 nm) at different positions to extract the nonlinear phase. The spectral signals and nonlinear phases are shown in Fig. 6. And the fitting results of nonlinear phases with wavelength resolutions of 0.1 nm and 0.8 nm are shown in Table 2. It can be seen from Table 2 that the thickness and refractive index of a wavelength resolution of 0.1 nm remain almost unchanged at different positions, whereas the fitting results with a wavelength resolution of 0.8 nm have an evident trend of changing with measuring position, i.e., the nonlinear phase changes with measuring position. However, the selection of the wavelength resolution of the spectrometer must consider factors such as the system cost and signal noise. And a spectrometer with wavelength resolution of 0.8 nm is used in our system, thus, the influence of the wavelength resolution must be reduced. Theoretically, the influence of wavelength resolution can be calibrated; however, the optical thickness of the measured film is unknown, i.e., the period of the recorded spectral signal is not fixed, and therefore the calibration process is complex and difficult. Because the influence of the wavelength resolution is the integral average effect on the intensity of spectral signal, so if the five-step phase-shifting algorithm is performed at the position where the spectral signal contains less periods, the influence will be weakened.

4. Experiments

4.1. System configuration

Figure 7 shows a schematic diagram of the white-light spectral interferometer used in our proposed method. A high-power halogen lamp with a central wavelength of 608 nm is used as the light source. The illumination arm is composed of Lens 1 and Lens 2, and an aperture diaphragm is built in to obtain a Köhler illuminator providing highly homogeneous illumination for both the sample and the reference mirror. The beam splitter (BS1) prism divides the incident light from illumination arm into two beams, which then enters the measuring and reference optical paths through two objective lenses. A 20X double-objective lens with a numerical aperture of 0.45 is used in this study. The measuring and reference beams are transmitted and reflected again through BS1, and subsequently interfere. A portion of beams is collected by a spectrometer with a wavelength resolution of 0.8 nm (QEPRO, Ocean Optics) via an optical fiber with a core diameter of 50 μm after passing through the beam splitter (BS2) prism. The other portion of beams collected by the camera can be used in the VSI method to reconstruct the surface topography. A lead zirconate titanate piezoelectric ceramics (PZT) actuator is used for vertical scanning and positioning. The entire measurement system is placed on an active vibration-isolation platform to avoid noise due to external vibration.

4.2. Measurement of SiO_2 film

We first measured a SiO_2 film on Si substrate with a thickness of 5.017 μm measured by the commercial reflectometry instrument for further illustration of the influence of wavelength resolution. Vertical scanning was performed with 10 nm steps when the scanning position was close to the top and bottom surfaces. The reconstructed interferometric signal of vertical scanning is shown in Fig. 8(a). We performed a five-step phase-shifting algorithm with the wavelength resolution of 0.8 nm at three different measuring positions (Position 1, Position 2, and Position 3 in Fig. 8(a)), and the extracted nonlinear phases are shown in Fig. 8(b). The measured nonlinear phase exhibits the same trend as the simulation results of Fig. 6, i.e., it also changes with the measuring position. Table 3 shows the fitting results of the thickness and effective refractive index of the nonlinear phase in Fig. 8(b), which implies that the measurement is sensitive to the change of nonlinear phases. The maximum percentage error is nearly 2.0% compared with

Optics EXPRESS

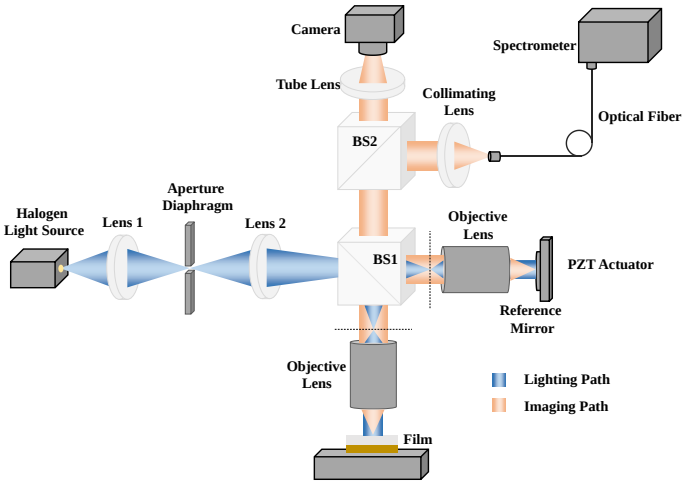

Fig. 7. Schematic diagram of white-light spectral interferometer.

the average value of theoretical refractive index in the wavelength bandwidth. The measured refractive index in Position 2 is within the theoretical value range of wavelength bandwidth, because the spectral signal contains less periods. Therefore, in the following measurement, the five-step phase-shifting algorithm is performed at the position where the spectral signal contains less periods, i.e., at the position where the zero optical path difference position is located near the middle of the top and bottom surfaces to reduce the influence of the wavelength resolution. The spectral signal of each frame of the five-step phase-shifting algorithm is repeatedly recorded and averaged to reduce the influence of vibrations from the environment.

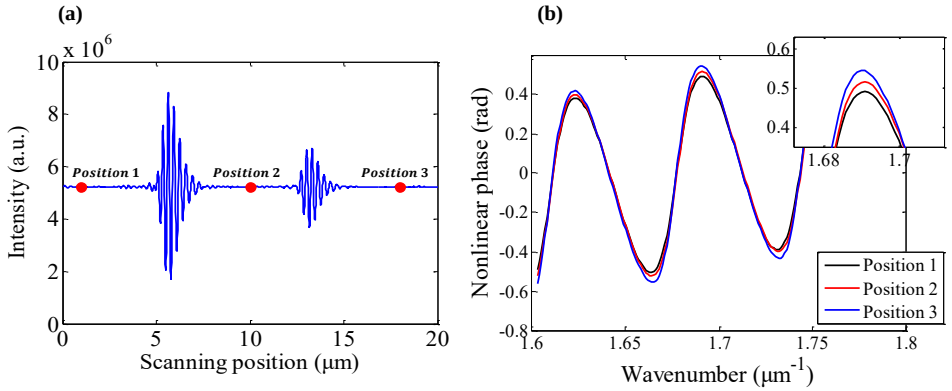

Fig. 8. (a) Reconstructed interferometric signal of vertical scanning, and (b) nonlinear phases at different measuring positions.

To experimentally verify the accuracy of the proposed method, we tested three SiO_2 films on Si substrate with thicknesses of 1.886, 5.017, and 10.068 μm measured by the commercial reflectometry instrument. A five-step phase-shifting algorithm was employed at the position where the zero optical path difference position is located near the middle of top and bottom surfaces to extract the nonlinear phase. The spectral signal of each frame of the five-step phase-shifting algorithm was repeatedly recorded by five times and averaged. For the measurement of

Optics EXPRESS

Table 3. Fitting results of nonlinear phases in Fig. 8(b)

Measuring position	Effective refractive index n_{eff}	Measured thickness d (μm)	Relative error (%)
Position 1	1.441	5.069	1.1
Position 2	1.459	5.001	0.0
Position 3	1.486	4.914	2.0

film thicknesses of 1.886, 5.017, and 10.068 μm, the wavelength bandwidths were 545–625 nm, 570–625 nm, and 590–625 nm, respectively, and the theoretical refractive index was approximately 1.457–1.460. The nonlinear phase error caused by the system was likewise eliminated. Then, we performed the vertical scanning process with 10 nm steps when the scanning position was close to the top and bottom surfaces, and recorded the spectral signal at each scanning step. The interferometric signal of vertical scanning was reconstructed by integrating the white-light spectral signals to calculate the constraints of nonlinear fitting. Then, the measured nonlinear phase and theoretical nonlinear phase obtained by the multiple reflection model were fitted with constraints to obtain the thickness and effective refractive index of film. The measured and theoretical nonlinear phases are shown in Fig. 9, and the fitting results of thicknesses and effective refractive index are shown in Table 4. The measured refractive index is within the theoretical value range of wavelength bandwidth, and the measured thicknesses are closely aligned with the values provided by the commercial instrument, such that they confirm the good accuracy of the proposed method for measuring the thickness and refractive index. Further, the SiO_2 film with a thickness of 5.017 μm was measured eight times, and the mean and standard deviation of fitting results are shown in Table 5. The measurement repeatability of effective refractive index can reach 10^{-3}, indicating good repeatability of the proposed method.

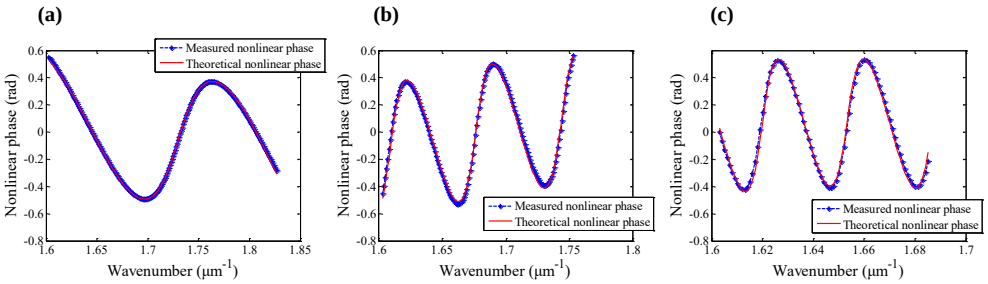

Fig. 9. Comparison between measured and theoretical nonlinear phases of film thicknesses of (a) 1.886 μm, (b) 5.017 μm, and (c) 10.068 μm.

Table 4. Fitting results of three SiO_2 films with different thicknesses

Thickness (μm)[a]	Effective refractive index n_{eff}	Measured thickness (μm)
1.886	1.457	1.885
5.017	1.459	5.011
10.068	1.458	10.059

[a]The thickness is measured by the commercial reflectometry instrument (F20-EXR, Filmetrics).

Optics EXPRESS

Table 5. Repeated measurement results of the SiO_2 film with thickness of 5.017 μm

	Effective refractive index n_{eff}	Measured thickness d (μm)
Mean	1.4596	5.0078
Standard deviation	0.0011	0.0042

4.3. Measurement of polymer film

The dispersion models of some polymer materials are unknown, or do not belong to the known dispersion model. Hence, for the film composed of mixed polymer materials, it is more difficult to measure the thickness and refractive index due to the uncertainty of the mixing ratio and the unknown chemical reaction. To demonstrate the feasibility of the proposed method, we measured a polymer film composed of several polymer materials on the *Si* substrate, which is used to encapsulate the wafer package. The measurement and fitting process are the same as described in Section 4.2. The measured and theoretical nonlinear phases with the wavelength bandwidth of 605–620 nm are shown in Fig. 10, and the fitting results of thickness and effective refractive index are shown in Table 6.

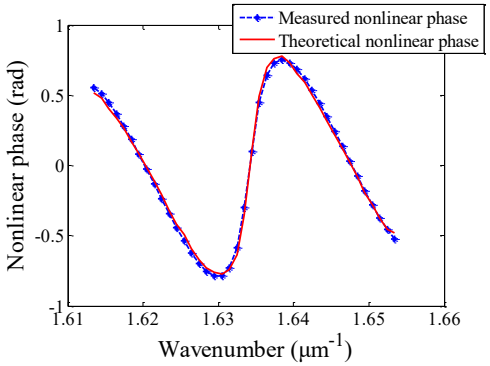

Fig. 10. Comparison between measured and theoretical nonlinear phases of the polymer film.

Table 6. Fitting results of the polymer film

	Effective refractive index n_{eff}	Measured thickness d (μm)
Polymer film	1.657	11.726

Because the dispersion model and initial values of thickness and refractive index of the polymer film are unknown, it is difficult to verify the measurement accuracy using commercial optical instruments. Hence, we used a stylus profiler to measure the height of the step structure at the film surface, i.e., the film thickness. The schematic diagram of the step structure is shown in Fig. 11(a), and the profile measurement result is shown in Fig. 11(b). Because the step structure is close to the edge of film, the surface is not flat. We selected a portion of data to calculate the step height, as shown by the red lines in Fig. 11(b). The profiles at three different positions were measured, and the average step height was 11.757 μm. Thus, the result of step height measured by the stylus profiler is consistent with the fitting result of the thickness in Table 6, which demonstrates that this method is feasible for measuring the film without a priori knowledge of the dispersion model and initial values of thickness and refractive index.

Optics EXPRESS

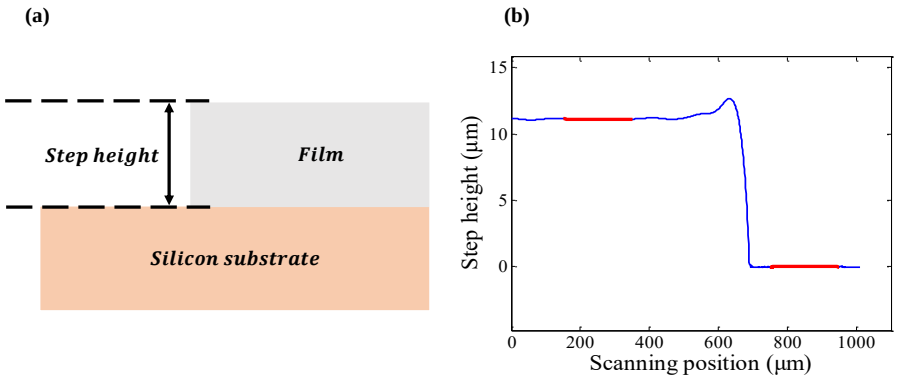

Fig. 11. (a) Schematic diagram of step structure, and (b) profile measured by a stylus profiler.

Meanwhile, the polymer film was measured using the VSI method, and the surface topography of top and bottom surfaces of film was reconstructed with the assistance of the fitting results of the proposed method, as shown in Fig. 12. The average thickness of the measurement area is calculated as 11.713 μm.

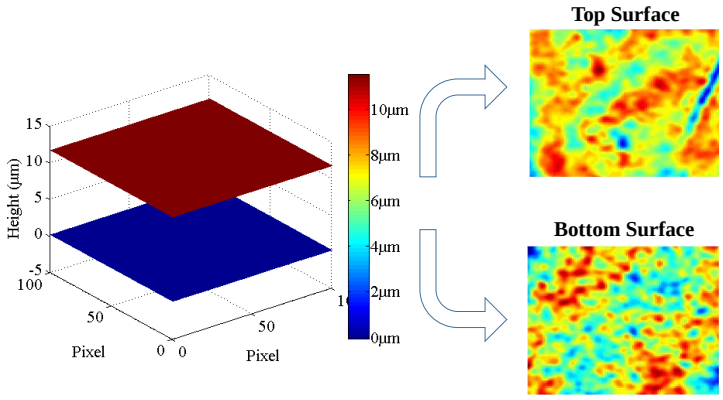

Fig. 12. Surface topography of top and bottom surfaces of polymer film.

5. Conclusion

We propose a constrained nonlinear fitting method for simultaneous measurement of the thickness and refractive index of film. The nonlinear phase extracted by the spectral phase-shifting is fitted with the theoretical nonlinear phase obtained by the multiple reflection model. More importantly, to avoid local minima, we establish two constraints using the interferometric signal of vertical scanning reconstructed by the integration of the white-light spectral signal. We describe the nonlinear fitting process with constraints in detail. Subsequently, the factors affecting the fitting results are analyzed, mainly including the constraints accuracy and wavelength resolution. Constraint 1 exhibits good accuracy and stability, as the gravity method is widely employed in coherence envelope detection. For Constraint 2, we simulate the measurement of a SiO_2 film

Optics EXPRESS

with different error percentages (0–10%) of T_1 and T_2. The results show that the fitting results of refractive index are within the error band of 1% of the theoretical value. Meanwhile, to reduce the influence of the integral average effect of the wavelength resolution, the five-step phase-shifting algorithm is performed at the position where the spectral signal contains less periods.

We measure three SiO_2 films with different thicknesses. The results show that the measured refractive index is within the theoretical value range of wavelength bandwidth, and the measured thicknesses are closely aligned with the values provided by the commercial instrument, which confirms the good accuracy of the proposed method. The repeated measurement is likewise carried out, and the measurement repeatability of refractive index can reach 10^{-3}. Furthermore, a polymer film composed of several polymer materials is measured, which is difficult to measure by some commercial optical instruments as the dispersion model and initial values of thickness and refractive index are unknown. The fitting result is verified by the step height measurement using a stylus profiler, further demonstrating the feasibility of the proposed method. The surface topography of top and bottom surfaces of the polymer film is reconstructed using the VSI method with the assistance of the fitting results of the proposed method. The most significant feature of the proposed method is that the measurement does not require a priori knowledge of the dispersion model and initial values of thickness and refractive index, and it is capable of assisting the VSI method in reconstructing the surface topography of top and bottom surfaces of the film because its system is compatible with the VSI method. In the proposed method, when the extinction coefficient of measured film is small, the equivalent calculation of refractive index may cause a large error in the measurement of extinction coefficient. Therefore, in future work, we will focus on the measurement of film with a large extinction coefficient and high dispersion. Research on the effects of surface and internal scattering on the measurement of optical constants of film will also be carried out.

Funding. National Key Research and Development Program of China (2017YFF0107000); 111 Project (B07014).

Disclosures. The authors declare no conflicts of interest.

Data availability. Data underlying the results presented in this paper are not publicly available at this time but may be obtained from the authors upon reasonable request.

References

1. J. Draper, I. Luzinov, S. Minko, I. Tokarev, and M. Stamm, "Mixed polymer brushes by sequential polymer addition: Anchoring layer effect," Langmuir **20**(10), 4064–4075 (2004).
2. K. N. Chen, C. A. Cheng, W. C. Huang, and C. T. Ko, "Bonding temperature optimization and property evolution of SU-8 material in metal/adhesive hybrid wafer bonding," J. Nanosci. Nanotechnol. **11**(8), 6969–6972 (2011).
3. E. M. A. Pereira, P. M. Kosaka, H. Rosa, D. B. Vieira, Y. Kawano, D. F. S. Petri, and A. M. Carmona-Ribeiro, "Hybrid materials from intermolecular associations between cationic lipid and polymers," J. Phys. Chem. B **112**(31), 9301–9310 (2008).
4. S. C. Qu and Y. Liu, "Stackable wafer-level analog chip-scale package," In: *Wafer-Level Chip-Scale Packaging*. Springer, New York, NY (2015).
5. J. A. Pradeep and P. Agarwal, "Determination of thickness, refractive index, and spectral scattering of an inhomogeneous thin film with rough interfaces," J. Appl. Phys. **108**(4), 043515 (2010).
6. P. Hlubina, J. Lunacek, and D. Ciprian, "The effect of silicon substrate on thickness of SiO_2 thin film analysed by spectral reflectometry and interferometry," Appl. Phys. B: Lasers Opt. **95**(4), 795–799 (2009).
7. K. Frank, "Urban III. Ellipsometry algorithm for absorbing films," Appl. Opt. **32**(13), 2339–2344 (1993).
8. V. A. Tolmachev, "Determining the thickness of thick transparent films by multiangle ellipsometry," J. Opt. Technol. **69**(1), 58–60 (2002).
9. R. Claveau, P. Montgomery, M. Flury, and G. Ferblantier, "Local inspection of refractive index and thickness of thick transparent layers using spectral reflectance measurements in low coherence scanning interferometry," Opt. Mater. **86**(1), 100–105 (2018).
10. H. L. Lee, S. H. Han, S. Y. Ana, W. Songa, O. Shina, and S. B. Kima, "Measurement of the refractive index of a transparent film using interferometry," Proc. SPIE **11056**, 10563J (2019).
11. M. C. Li, D. S. Wan, and C. C. Lee, "Application of white-light scanning interferometer on transparent thin-film measurement," Appl. Opt. **51**(36), 8579–8586 (2012).
12. K. Kitagawa, "Surface and thickness profile measurement of a transparent film by three-wavelength vertical scanning interferometry," Opt. Lett. **39**(14), 4172–4175 (2014).

Optics EXPRESS

13. Y. Arosa, E. L. Lago, and R. D. L. Fuente, "Refractive index retrieval in the UV range using white light spectral interferometry," Opt. Mater. **82**(1), 88–92 (2018).
14. Y. Arosa, E. L. Lago, and R. D. L. Fuente, "The phase ambiguity in dispersion measurements by white light spectral interferometry," Opt. Laser Technol. **95**(1), 23–28 (2017).
15. Y Arosa and R. D. L. Fuente, "Refractive index spectroscopy and material dispersion in fused silica glass," Opt. Lett. **45**(15), 4268–4271 (2020).
16. Q. K. Zhang, S. C. Zhong, J. F. Zhong, and X. B. Fu, "Ultrahigh-accuracy measurement of refractive index curves of optical materials using interferometry technology," Meas. **122**(1), 40–44 (2018).
17. J. Jin, J. W. Kim, C. S. Kang, J. A. Kim, and T. B. Eom, "Thickness and refractive index measurement of a silicon wafer based on an optical comb," Opt. Express **18**(17), 18339–18346 (2010).
18. K. Zhang, L. Tao, W. K. Cheng, J. H. Liu, and Z. P. Chen, "Interference enhancement in spectral domain interferometric measurements on transparent plate," Appl. Opt. **53**(26), 5906–5911 (2014).
19. Y. S. Ghim and S. W. Kim, "Thin-film thickness profile and its refractive index measurements by dispersive white-light interferometry," Opt. Express **14**(24), 11885–11891 (2006).
20. T. Guo, Z. Chen, M. H. Li, J. H. Wu, X. Fu, and X. T. Hu, "Film thickness measurement based on nonlinear phase analysis using a Linnik microscopic white-light spectral interferometer," Appl. Opt. **57**(12), 2955–2961 (2018).
21. T. Guo, G. H. Zhao, D. W. Tang, Q. W. Weng, C. B. Sun, F. Gao, and X. Q. Jiang, "High-accuracy simultaneous measurement of surface profile and film thickness using line-field white-light dispersive interferometer," Opt. Lasers Eng. **137**(1), 106388 (2021).
22. S. Debnath, M. P. Kothiyal, J. Schmit, and P. Hariharan, "Spectrally resolved white-light phase-shifting interference microscopy for thickness-profile measurements of transparent thin film layers on patterned substrates," Opt. Express **14**(11), 4662–4667 (2006).
23. T. Guo, L. Yuan, Z. Chen, M. H. Li, X. Fu, and X. T. Hu, "Single point Linnik white-light spectral microscopic interferometer for surface measurement," Surf. Topogr.: Metrol. Prop. **6**(3), 034008 (2018).